J E M T
Journal of Earth and Marine Technology
homepage URL: ejurnal.itats.ac.id/jemt

Impact of Land Subsidence-Induced Three-Dimensional Surface Deformation on Infrastructure in the Semarang-Demak Alluvial Plain, Indonesia

Reyhan Azeriansyah*[1], Kuo-En Ching[1], Bambang Darmo Yuwono[2]
[1] Department of Geomatics, National Cheng Kung University, Taiwan
[2] Department of Geodetic Engineering, Universitas Diponegoro, Indonesia
*e-mail: p68097072@gs.ncku.edu.tw

Article info
Received:
Dec 16, 2024
Revised:
Jan 6, 2025
Accepted:
Jan 8, 2025
Published:
March 14, 2025

Keywords:
Land subsidence, SBAS-InSAR, Mogi Source Model, Groundwater extraction, Surface deformation.

Abstract

We estimated surface deformation using SBAS-InSAR and the Mogi Source Model is then adopted to elucidate the mechanisms and spatial variability of surface deformation within the Semarang-Demak Alluvial Plain and its impacts on infrastructures. By analyzing predicted vertical and horizontal velocities, we identify intensive groundwater extraction as the primary driver of aquifer compaction, with vertical subsidence exceeding -120 mm/year and volume loss rates surpassing -6,000 m^3/year in the urbanized Semarang-Demak region. These findings highlight the three-dimensional characteristics of deformation, forming a characteristic "bowl-shaped" pattern and revealing the sensitivity of infrastructure—expressways, railways, national roads, local roads, and airports—to high strain and tilt gradients. The integrated analysis thus underscores the necessity of sustainable groundwater management and adaptive land-use strategies to mitigate deformation-induced risks. This approach is crucial for safeguarding the long-term functionality and resilience of vital infrastructure in this subsidence-prone coastal region, guiding decision-makers toward strategic and sustainable development practices.

1. Introduction

Land subsidence has emerged as a critical environmental challenge in many coastal and low-lying regions worldwide, including Indonesia [1], [2], [3]. In the Semarang-Demak region, excessive groundwater extraction, combined with tectonic activity and sediment consolidation, has also caused significant surface deformation [4], [5]. This heterogeneous deformation disrupts urban infrastructure, damaging buildings, roads, and drainage systems, while also exacerbating flooding, saltwater intrusion, and the depletion of groundwater resources [6]. As the region experiences rapid economic development and increasing urban demands, a comprehensive understanding of surface deformation dynamics is essential to support sustainable groundwater management, urban planning, and infrastructure resilience.

Vertical displacement determined by geodetic data has been primarily focused in Semarang and its surrounding areas in previous studies [1], [6], [7], [8]. However, vertical subsidence measurements alone may not fully capture the complexities of ground movement, which often involves significant horizontal components [9]. Neglecting these subtle but critical horizontal displacements can lead to incomplete understanding of surface deformation processes. By integrating both vertical and horizontal ground motions, a more accurate and multidimensional assessment of subsidence mechanisms can be achieved. Such insights are crucial for identifying the underlying processes driving land subsidence induced by groundwater extraction and predicting 3D deformation patterns.

Recent advancements in remote sensing technologies, particularly Interferometric Synthetic Aperture Radar (InSAR), have revolutionized our ability to monitor and quantify ground deformation with high spatial and temporal resolution [10], [11]. Among InSAR techniques, the Small Baseline Subset (SBAS) approach has demonstrated its effectiveness in producing detailed and reliable measurements of surface displacement [12]. By combining with physics-based deformation models, such as the Mogi Source Model, observed surface changes can be more accurately attributed to specific subsurface processes [13], [14]. This integrated approach combines high-spatial-resolution remote sensing data with

analytical models, enhancing our predictive capabilities for surface deformation and providing valuable insights for mitigation efforts.

This study aims to predict surface deformation induced by groundwater pumping in the Semarang-Demak Alluvial Plain through the integration of SBAS-InSAR method and analytical deformation modeling. By incorporating both vertical and horizontal displacement components and utilizing physics-based models, we provide a comprehensive understanding of the mechanisms driving land subsidence and its implications for infrastructures. Subsequently, the outcomes of this study will serve as a critical foundation for formulating evidence-based groundwater management policies, optimizing infrastructure design, and guiding sustainable urban development in subsidence-prone coastal environments. Furthermore, the results in this research contribute to the broader efforts to enhance the resilience and stability of coastal urban regions facing ongoing environmental and socioeconomic challenges.

2. Methodology

2.1. InSAR data processing and validation

This study utilized synthetic aperture radar (SAR) data from the Sentinel-1 satellite, provided by the European Space Agency (ESA) via the COMET-LiCS Sentinel-1 InSAR web portal (https://comet.nerc.ac.uk/COMET-LiCS-portal/). The study area covered approximately 250 × 250 km, spanning the Semarang-Demak alluvia plain regions, using the interferometric wide (IW) swath mode with descending track (076D) (Figure 1). The Sentinel-1 data were characterized by an incidence angle (θ) of about 33.802° and a heading angle (α) of approximately –167.493°. A total of 775 interferometric pairs acquired between January 2015 and March 2024 were analyzed. Data processing was carried out using the open-source LiCSBAS InSAR time-series analysis package, developed by Morishita et al. [15], which integrates directly with LiCSAR products. The workflow began with downloading unwrapped interferograms and coherence maps in GeoTIFF format, which were then converted to a compatible binary format for further processing. Atmospheric phase delays, primarily caused by tropospheric water vapor variability, were mitigated using tropospheric correction maps from the Generic Atmospheric Correction Online Service for InSAR (GACOS), which significantly reduced the impact of atmospheric noise on the interferometric phase [16], [17].

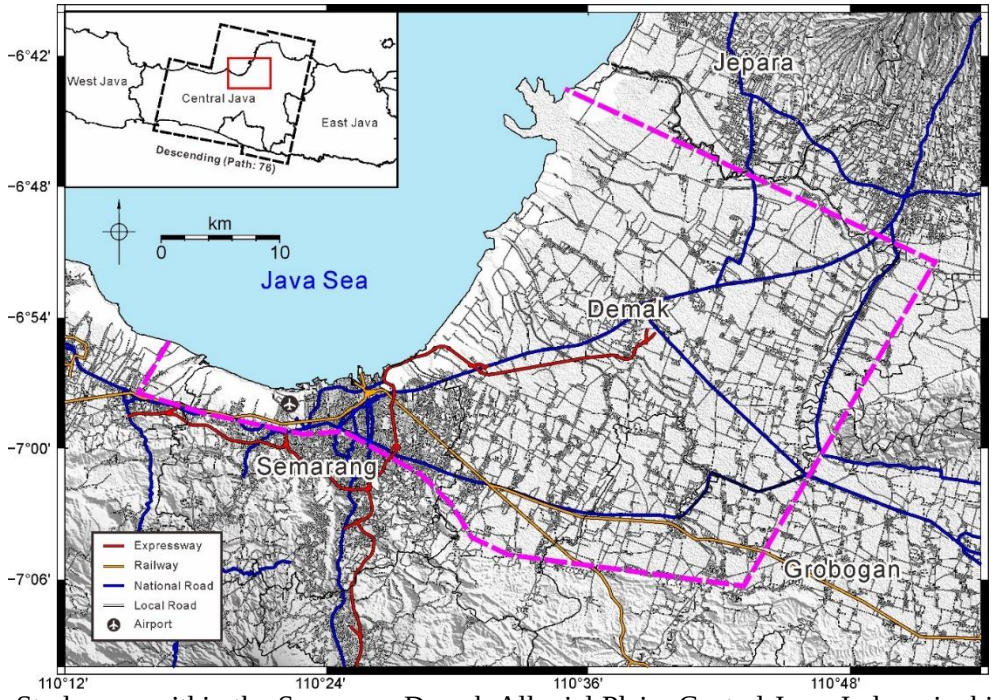

Figure 1. Study area within the Semarang-Demak Alluvial Plain, Central Java, Indonesia, highlighted by the purple dashed line. The map illustrates key infrastructure, including expressways (red lines), railways (orange lines), national roads (blue lines), local roads (light gray lines), and the airport (denoted by an airplane symbol). The inset map in the upper-left corner indicates the location of the study area within Central Java and the extent of InSAR data coverage, represented by the black dashed rectangle.

The quality of the interferometric network was refined through automated loop closure analysis to identify and exclude interferograms containing phase unwrapping errors, ensuring that only high-quality data were used for subsequent analysis. A small baseline (SB) network inversion method was then applied to derive incremental displacements between acquisition epochs. These incremental displacements were integrated to produce cumulative displacement time series, while the mean line-of-sight (LOS) velocity was estimated through least-squares regression. To further suppress residual noise, including atmospheric artifacts and orbital errors, a spatiotemporal Gaussian filter was applied. This filtering process effectively reduced high-frequency noise while preserving signals of interest, such as surface deformation trends.

The final outputs, including LOS displacement time series and velocity maps, were carefully analyzed and visualized. Masking based on coherence values, velocity standard deviation, and other noise indices was implemented to exclude unreliable pixels and enhance result accuracy [15]. To ensure the reliability and accuracy of the SBAS-InSAR results, the data were referenced and validated using continuous GNSS data from the Continuous Operating Reference Station (CORS) network managed by the Indonesian Geospatial Information Agency (BIG) (https://srgi.big.go.id/) [18]. The reference point for the SBAS-InSAR analysis was set to the CORS located in Semarang (CSEM), serving as a stable geodetic reference which has shown no substantial deformation. Validation was performed by comparing the InSAR LOS velocity with the GNSS observations using Equation 1 [19], [20]:

$$V_{LOS}^{D} = \begin{bmatrix} -\sin\theta^{D}\cos\alpha^{D} & \sin\theta^{D}\sin\alpha^{D} & \cos\theta^{D} \end{bmatrix} \begin{bmatrix} V_E \\ V_N \\ V_U \end{bmatrix} \quad (1),$$

where V_{LOS}^{D} represents the LOS velocity of InSAR descending orbit. θ^{D} respresents the descending looking angle, α^{D} represents the descending heading angle, V_E, V_N, V_U represent the GNSS-derived velocities in the easting, northing, and vertical (up) components, respectively.

2.2. Mogi Source Modeling for Groundwater Extraction-Induced Deformation

As land subsidence is caused by layer compaction, we utilize the Mogi Source Model to invert InSAR LOS velocities in this study, estimating the volume changes of point sources as the equivalent effects of layer compaction and then calculating the resulting three-dimensional surface deformation (Figure 2). The Mogi model provides a theoretical framework for describing surface deformation induced by a point source (or spherical pressure source) embedded in an elastic half-space [13]. It is particularly effective for simulating deformation due to subsurface volumetric changes, such as those caused by fluid extraction, magma chamber pressurization, or aquifer compaction [14], [21], [22]. The Mogi Source Model relates surface displacements to a spherical pressure source and is given in Equation 2 as follows:

$$\begin{pmatrix} V_E \\ V_N \\ V_U \end{pmatrix} = \Delta V \frac{(1-\gamma)}{\pi} \begin{pmatrix} \frac{x}{R^3} \\ \frac{y}{R^3} \\ \frac{d}{R^3} \end{pmatrix} \quad (2),$$

where V_E, V_N, V_U are the surface velocities in the easting, northing, and up directions, respectively, ΔV is the average volume change of the source (m³/year), γ is Poisson's ratio that characterizes the elastic properties of the medium, 0.25, x and y are the coordinates of the possible groundwater extraction location, d is the burial depth of the source, with positive values denoting the distance downward from the ground in the study area, and R is the radial distance from the subsurface source to the observation points. In this study, we implemented a multi-source scenario to estimate the spatial distribution of the layer volume change rates in the subsidence area of Semarang-Demak Alluvial Plain. This targeted approach ensures that the analysis focuses on regions where groundwater extraction has a measurable impact on ground deformation. The process utilized input from InSAR LOS velocity descending orbit resampled to a grid size of 500 × 500 m to balance spatial detail with computational efficiency, ensuring sufficient coverage and accuracy in areas most affected by subsidence.

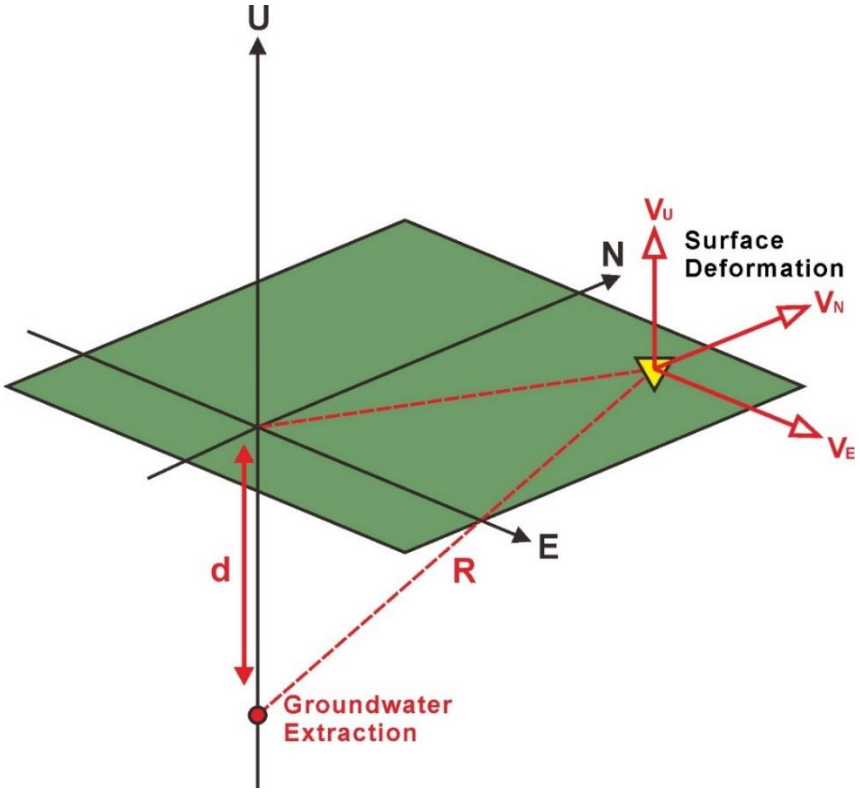

Figure 2. Conceptual model of Mogi Source Model for land subsidence.

In this approach, the possible locations of layer compaction are divided into a grid with a spacing of 250 × 250 m, and each grid node is treated as a potential deformation source. The depth (d) was fixed at 120 m, reflecting the typical groundwater extraction range in Semarang, which occurs between 60 and 180 m [23]. The estimation of ΔV was performed using a weighted least-squares inversion to minimize the residuals between the observed surface deformation and the deformation predicted by the Mogi Source Model. The inversion system is expressed as Equation 3:

$$\begin{bmatrix} WG_{InSAR} \\ \kappa^2 \nabla^2 \end{bmatrix} [m_{\Delta V}] = \begin{bmatrix} Wd_{InSAR} \\ 0 \end{bmatrix} \quad (3),$$

where WG is the weighted Green's function for the design matrix consisting of the shape function for InSAR, κ^2 is the smoothing factor that determines the Laplacian smoothing, ∇^2 is the discretized approximation of the Laplacian smoothing operation [24], and Wd is the weighted InSAR velocity coefficient matrix derived from the SBAS-InSAR data process. The weighting matrix W combines two weighting schemes: uncertainty-based weighting derived from the standard deviations of the InSAR LOS velocities, where observations with smaller uncertainties, which are more reliable, are assigned higher weights. This ensures that high-quality data contribute more significantly to the inversion results. The distance-based weighting is applied to prioritize observations closer to each grid node. The distance-based weight is defined by Equation 4:

$$W_{dist} = \frac{1}{1+\left(\frac{\sqrt{dx^2+dy^2}}{\sigma}\right)} \quad (4),$$

where dx and dy are the distances between the point source of layer compaction and the InSAR observation points, and σ is the distance-decay constant. We selected a distance decay constant of 1,000 m to reflect the gradual reduction in deformation sensitivity with distance from the compaction source, ensuring relatively high weights for nearby observations while retaining contributions from distant data to maintain spatial continuity and solution stability. A critical focus in our model is selecting and applying the smoothing factor, κ^2. To achieve optimal model performance, we conducted a trade-off analysis by evaluating κ^2 values ranging from 0 to 1.0. The evaluation process involved assessing the model performance using the root-mean-square (RMS) misfit, which quantifies the discrepancy between observed and modeled values. The selected κ^2 value corresponded to the point where the RMS misfit

was minimized, ensuring an optimal compromise between model fidelity to local variations and its ability to generalize across the dataset. After we obtained the optimal ΔV, we estimated the predicted horizontal and vertical velocities in the subsidence-affected regions using the Mogi Source Model. The predicted horizontal velocities ($\hat{V}_E$ and $\hat{V}_N$) and vertical velocities ($\hat{V}_U$) are derived based on the spatial distribution of the estimated ΔV and the geometric relationships between the source location and observation points. Following the estimation of horizontal and vertical velocity components, strain analysis was conducted to characterize the spatial distribution and intensity of deformation and its potential impact on overlying infrastructure. By integrating the vertical and horizontal motion fields, the second invariant and tilt rates were derived [25], [26], [27]. These quantitative deformation indicators a robust basis for assessing the vulnerability of infrastructure within the Semarang-Demak Alluvial Plain. The second invariant measures the overall strain intensity, highlighting regions with concentrated stress that may lead to structural damage, while the tilt rate captures surface inclination changes that indicate potential misalignment and instability. Together, these metrics offer a comprehensive understanding of deformation mechanisms and their implications for infrastructure resilience.

3. Results and Discussion

3.1. *LOS surface deformation pattern derived from InSAR*

The validation of InSAR-derived LOS velocities in this study was performed using data from seven regional CORSs, which yielded an accuracy of approximately 3–5 mm/year, indicates a general consistency between the InSAR and GNSS-derived deformation measurements at a regional scale. However, the spatial distribution of the regional CORSs, which are located outside the immediate boundary of the Semarang-Demak Alluvial Plain (Figure 3), introduces limitations in capturing localized deformation. The Semarang-Demak Alluvial Plain is characterized by highly variable subsidence, influenced by local factors such as groundwater extraction and sediment compaction. Due to the large spacing between CORSs, they primarily capture large-scale surface deformation, particularly tectonic deformation, and are unable to resolve the spatial heterogeneity of ground motion within the plain. In addition, InSAR LOS velocities represent total ground movement projected onto the radar line of sight, inherently combining vertical subsidence with potential horizontal motion. Therefore, obtaining true 3D surface deformation using conventional methods mainly requires relying on high-density geodetic observations, such as leveling surveys or GNSS observations. However, the spatial resolution of these conventional methods is significantly lower than that of InSAR. To achieve true 3D surface deformation, estimate while retaining the high spatial resolution of InSAR, we employ the Mogi Source Model to derive three-dimensional surface deformation with the spatial resolution of InSAR in this study.

The LOS surface deformation velocities derived from InSAR data across the Semarang-Demak Alluvial Plain reveal a clear west-to-east gradient in ground displacement. The western part of the alluvial plain, particularly in the Semarang-Demak region, experiences the most severe LOS deformation, with velocities reaching up to -120 mm/year (Figure 3). Moving eastward toward the Demak region, deformation rates gradually decrease to -40 mm/year. The observed deformation pattern indicates that subsidence dominates as the primary motion in this area, though minor contributions from horizontal movement. The significant subsidence observed in the western part of the alluvial plain is primarily attributed to the compaction of unconsolidated sediment layers and anthropogenic activities, such as groundwater extraction and infrastructure loading. These activities are particularly prevalent in urban areas and are driven by general public use and industrial demands. In contrast, the relatively slower deformation rates in the central to eastern parts of the plain likely reflect variations in sediment characteristics and lower levels of anthropogenic activity. The uncertainty of the InSAR LOS velocity reveals spatial variability across the study area, with values ranging from 0.1 to 0.5 mm/year (Figure 4). Given the low uncertainty, the InSAR-derived LOS velocities for the Semarang-Demak Alluvial Plain are considered reliable for identifying deformation patterns and quantifying subsidence rates. The spatial coverage and precision of InSAR offer a clear advantage for observing surface deformation across the study area.

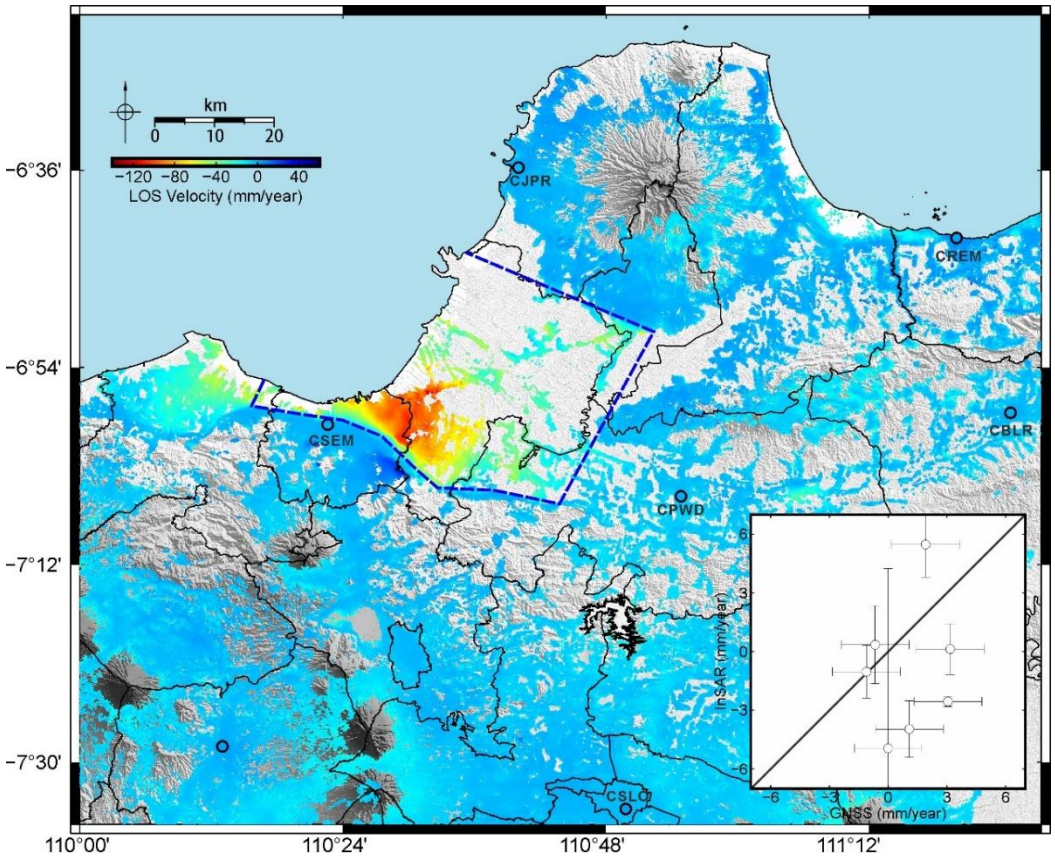

Figure 3. LOS velocities derived from InSAR data, with a comparison between InSAR and GNSS LOS velocities using regional CORSs. The velocities are presented relative to the reference point at CSEM.

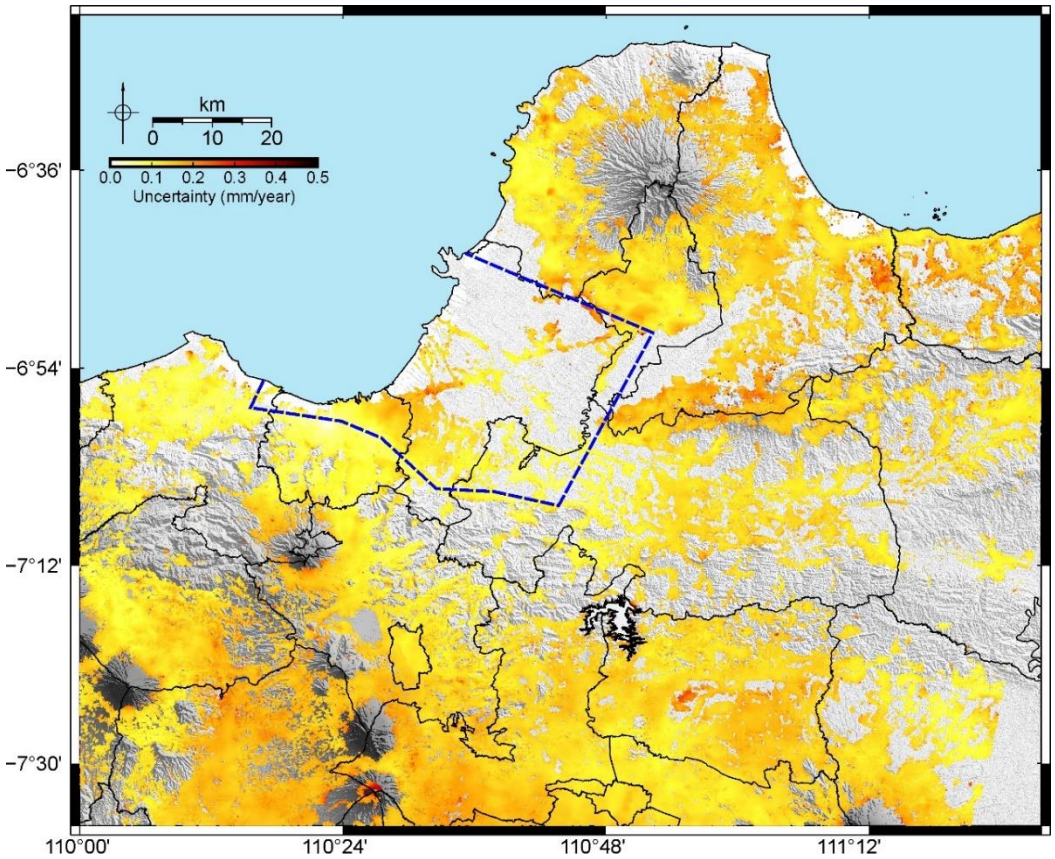

Figure 4. Uncertainty of LOS velocity derived from InSAR data

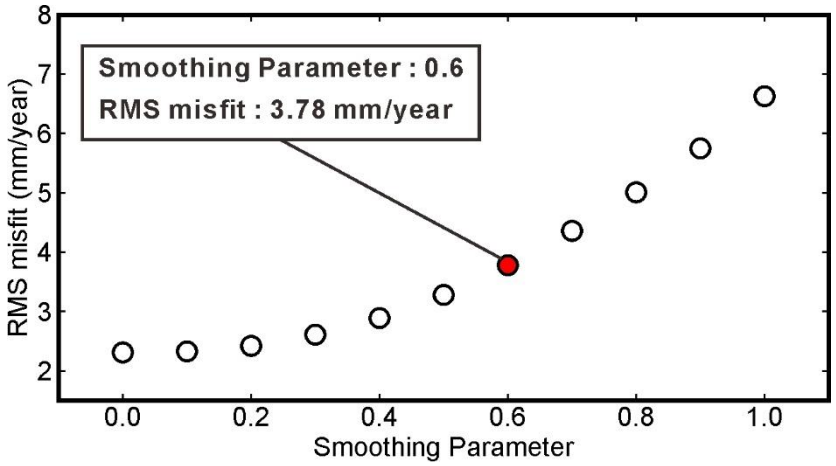

Figure 5. Relationship between the smoothing parameter and RMS misfit (mm/year) for selecting the optimal smoothing parameter

3.2. Groundwater extraction-induced deformation and its impacts on infrastructures

The analysis in this section investigates the surface deformation resulting from groundwater extraction-induced volume changes using the Mogi Source Model. The results are presented in terms of subsidence magnitudes, spatial distribution of volumetric changes, and associated deformation parameters derived from InSAR LOS velocities. This approach provides both qualitative and quantitative insights into the relationship between layer compaction and surface displacement patterns across the Semarang-Demak Alluvial Plain. The RMS misfit (Figure 5) evaluates the model performance in balancing the fidelity to observation and spatial smoothness. By assessing various smoothing parameters (κ^2) in the range of 0.0 to 1.0, the optimal smoothing parameter of 0.6 is identified, corresponding to an RMS misfit of 3.8 mm/year. This result demonstrates a reasonable compromise, where the residuals between the observed InSAR LOS velocities and the modeled deformation are minimized while avoiding overfitting. The selected parameter ensures that the Mogi Source Model adequately reflects the subsurface volume changes responsible for the observed deformation.

The calculated deformation (Figure 6B) derived from the Mogi Source Model reproduces the observed InSAR LOS velocities (Figure 6A) with notable accuracy. The calculated deformation field captures the high-subsidence zones in Semarang and the decreasing subsidence trend toward Demak, consistent with the spatial patterns seen in the observations. The residual map (Figure 6C) which represents the difference between the observed and modeled LOS velocities, indicates minimal discrepancies in most regions. The residuals are relatively small, generally within ±10 mm/year, confirming that the Mogi Source Model effectively simulates the surface deformation caused by subsurface volume changes. The results provide a quantitative measure of groundwater extraction-induced volumetric changes (Figure 6D), with rates exceeding -6,000 m³/year in the most subsidence-prone areas of the urban Semarang-Demak region. These high-volume loss zones coincide spatially with regions experiencing extreme LOS velocities, reinforcing the role of groundwater extraction in driving aquifer compaction and surface subsidence. Moving eastward, the volume loss rates progressively decrease to near-zero values, corresponding to areas with lower subsidence rates and reduced groundwater withdrawal activities. This spatial distribution highlights the relationship between groundwater extraction intensity and the resulting subsurface volumetric contraction. The findings are further supported by Abidin et al. [1] who demonstrated a clear relationship between land subsidence and the increasing number of registered groundwater wells. Their study showed that land subsidence rates tend to rise in conjunction with the number of wells, where a single groundwater well has the potential to extract approximately 9,000 to 36,000 m³/year. This significant water extraction can lead to substantial aquifer compaction, which, in turn, results in surface subsidence.

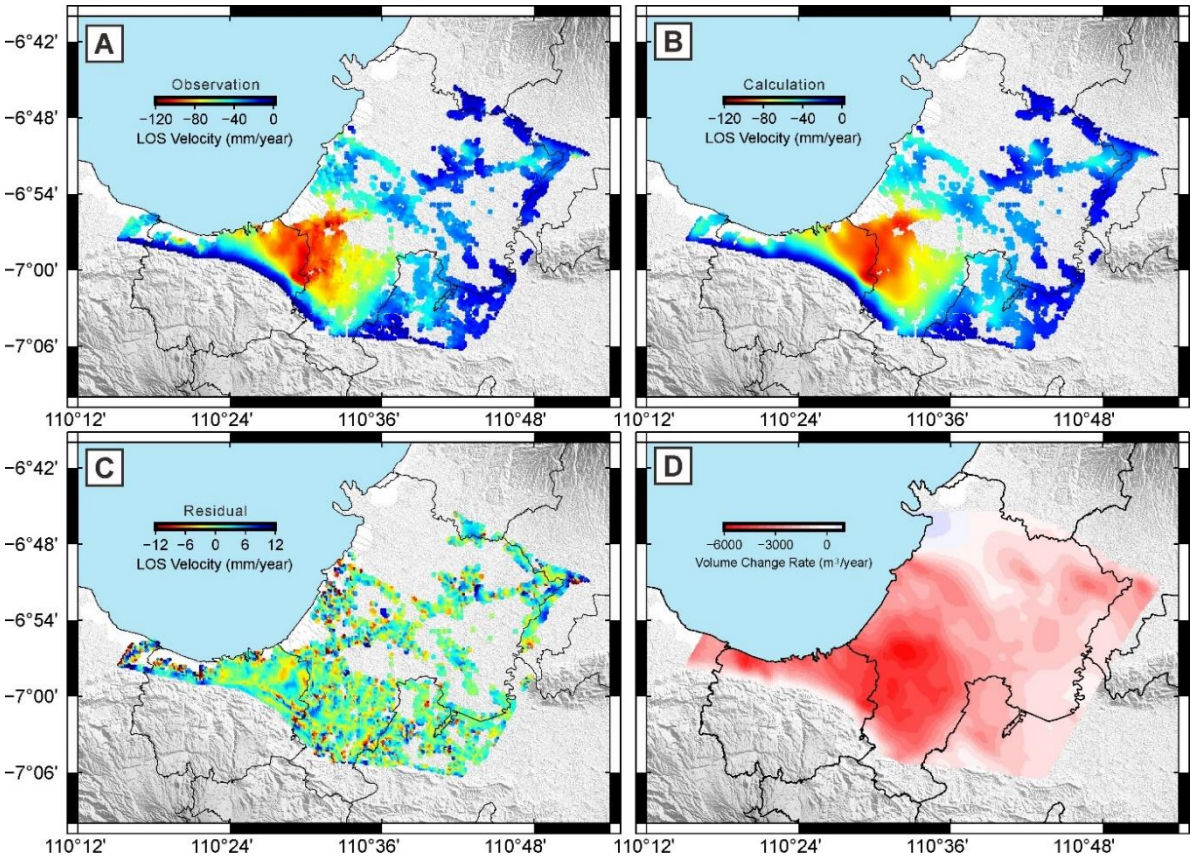

Figure 6. (A) LOS velocity observation, (B) LOS velocity calculation, (C) LOS velocity residual, and (D) Volume change rate (m^3/year) estimated from the Mogi source model.

The predicted vertical and horizontal velocities (Figure 7), derived from the Mogi Source Model, illustrate the deformation field induced by volumetric changes resulting from layer compaction. The vertical velocities, ranging from -120 mm/year to 0 mm/year, closely align with the spatial patterns observed in the InSAR LOS velocities, confirming that vertical ground displacement is the dominant deformation pattern. The most significant vertical subsidence is concentrated in the urbanized area of the western part of the alluvial plain, particularly in the Semarang-Demak region, where intensive groundwater extraction drives aquifer compaction, as evidenced by the maximum volumetric loss rates in the model. Horizontal velocity vectors indicate inward radial displacements directed toward the zones of maximum subsidence, representing the surface response to volumetric contraction at depth, as predicted by the Mogi Source Model. The magnitudes of the horizontal velocities decrease with increasing distance from the subsidence center, reflecting the diminishing influence of the deformation source. The combined vertical and horizontal displacements form a characteristic "bowl-shaped" deformation pattern, where the vertical displacement is greatest at the center and horizontal motion converges inward (Figure 7). This deformation geometry effectively visualizes the ground response to groundwater extraction and highlights groundwater compaction as the primary mechanism driving surface deformation in the Semarang-Demak Alluvial Plain.

To better identify potential areas where differential 3D surface velocity fields could cause damage to infrastructure, we further utilized the predicted horizontal and vertical velocities to estimate the second invariant and tilt rates, respectively. Based on the second invariant (Figure 8) and tilt rate (Figure 9), these analyses reveal significant impacts on key infrastructure systems, including railways, national roads, expressways, local roads, and the airport. The second invariant values, ranging from 0 to 15 × 10^{-6}/year, highlight zones of high strain intensity in the central and eastern parts of Semarang and extending into central and northern Demak, while tilt rate, reaching up to 50 × 10^{-6}/year, show steep gradients concentrated in coastal Semarang and central parts of Demak (Figure 8 and 9). These deformation patterns align spatially with critical infrastructure networks, posing risks of track misalignment, pavement cracking, and surface tilting.

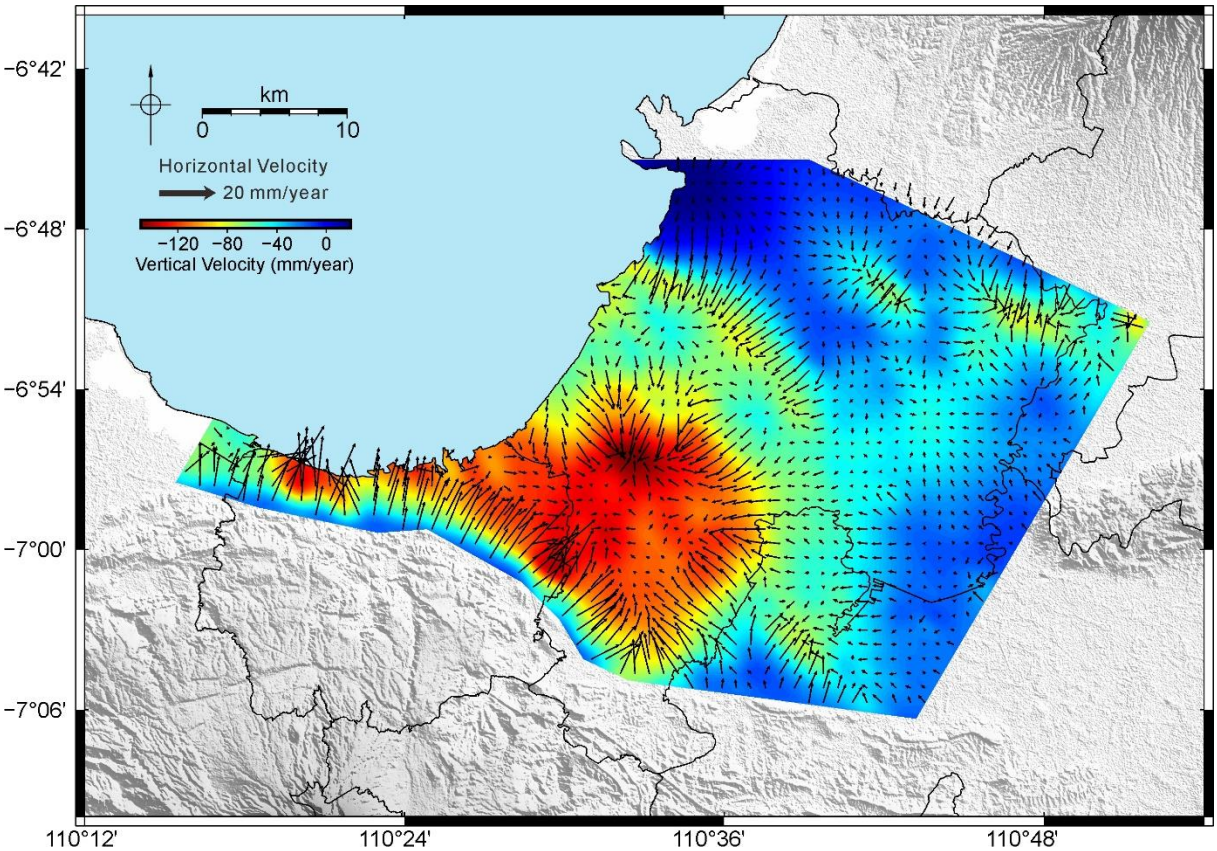

Figure 7. Predicted horizontal and vertical velocities derived from the Mogi Source Model

The railway systems in Semarang, Demak, and Grobogan are among the most affected, with concentrated strain and tilt gradients leading to subgrade instability and potential operational disruptions (Figure 8 and 9). Similarly, national roads in central to eastern Semarang and central Demak exhibit surface warping and localized pavement distress, further exacerbated by moderate yet abrupt deformation gradients. In urbanized areas, local roads in coastal Semarang and Demak are particularly vulnerable to surface cracking, differential settlement, and warping due to localized peaks in strain and tilt rates (Figure 8 and 9). The newly constructed expressways connecting Semarang and Demak experience more moderate impacts but remain susceptible to pavement distortion and uneven settlement in areas where tilt gradients intensify (Figure 9). The airport in Semarang exhibits a unique sensitivity to tilt rates, as even slight tilting of runway and taxiway surfaces compromises the precision required for safe take-off and landing operations (Figure 9). Although strain values at the airport remain moderate, the presence of steep tilt gradients necessitates continuous monitoring and timely interventions to mitigate operational risks (Figure 8).

To address these challenges, frequent monitoring using geodetic observation (e.g., leveling, GNSS, and InSAR) and subsurface observation methods (e.g., extensometers and multi-layer compaction monitoring wells) is critical for early detection of deformation. Routine inspections, immediate repair, and reinforcement should target high-risk infrastructure such as railways, roads, and airport. Long-term measures include regulating groundwater extraction, enhancing soil stability through engineering techniques, and adapting infrastructure designs to accommodate ongoing deformation.

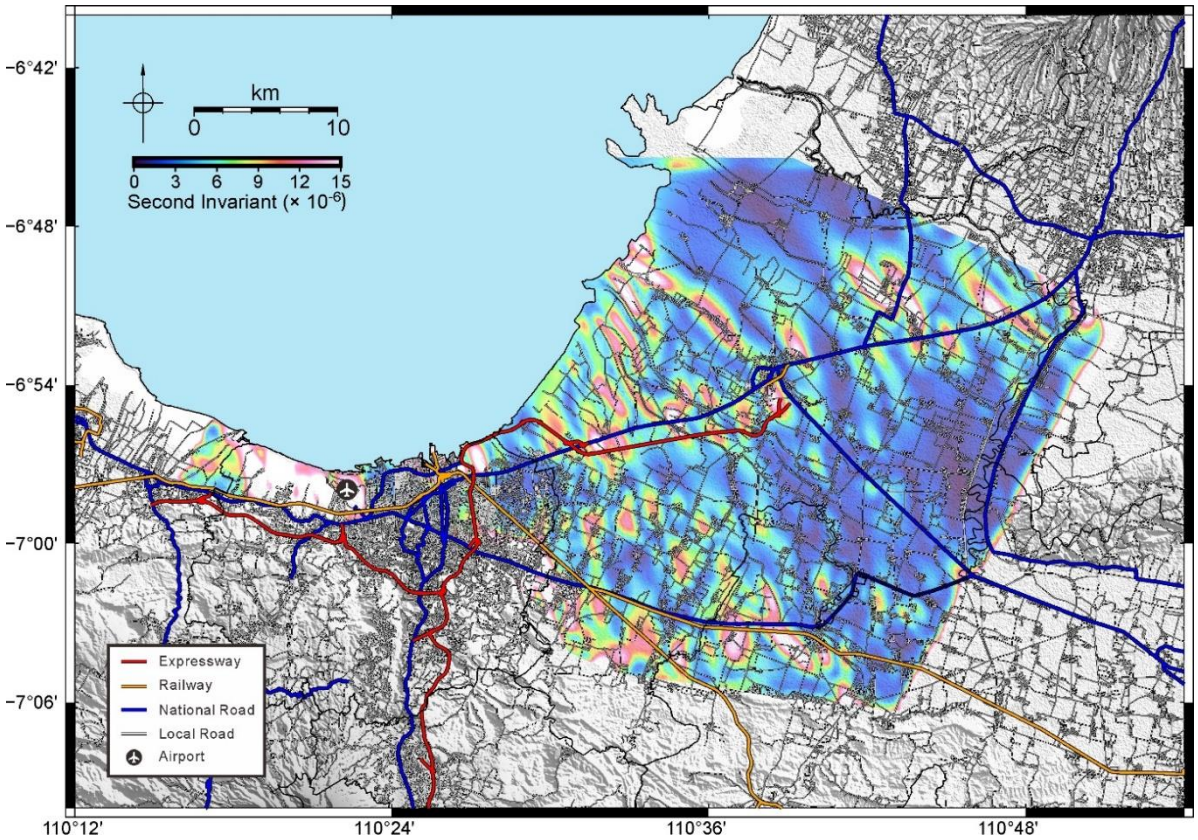

Figure 8. Spatial distribution of the second invariant in the Semarang-Demak Alluvial Plain, highlighting regions of high strain that can could lead to differential deformation of infrastructure, potentially causing damage.

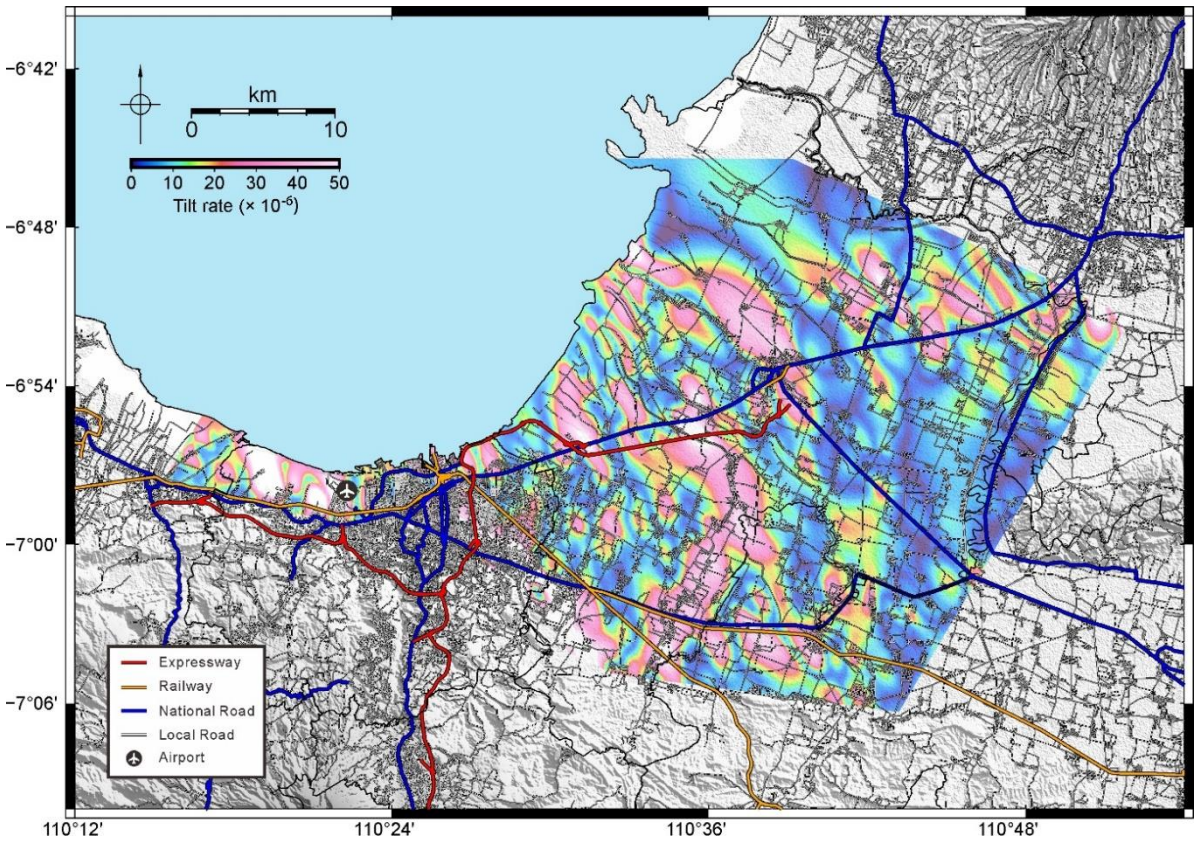

Figure 9. Spatial distribution of tilt rate in the Semarang-Demak Alluvial Plain, showing areas with steep tilt gradients that can cause surface tilting and misalignment in infrastructure.

4. Conclusions

The combination of SBAS-InSAR observations and the Mogi Source Model to thoroughly characterize ground deformation in the Semarang-Demak Alluvial Plain, providing a detailed understanding of both vertical and horizontal displacement fields. The results indicate that intensive groundwater extraction is the primary driver of widespread land subsidence, with rates exceeding -120 mm/year in the urbanized area of the western part of the alluvial plain, particularly in the Semarang-Demak region. Additionally, volume change rates surpassing -6,000 m^3/year confirm that aquifer compaction significantly contributes to these surface displacements. Such findings underscore the necessity for sustainable groundwater management to mitigate ongoing deformation, as well as the importance of integrating vertical and horizontal measurements for a more comprehensive assessment of subsidence mechanisms. The analyses of the second invariant and tilt rates further illuminate how infrastructure stability is influenced by deformation patterns. Major expressways, railways, and aviation facilities align with high-strain and steep-tilt zones, rendering them vulnerable to cracking, settlement, and leveling issues. Even moderately affected areas, such as national and local roads, are not immune to incremental damage over time. By combining geodetic data, analytical modeling, and deformation metrics, this research equips policymakers, urban planners, and engineers with the insights needed to enhance infrastructure resilience and inform more strategic, sustainable development practices in this subsidence-prone coastal region.

Acknowledgment

We extend our heartfelt appreciation to our co-authors for their invaluable contributions and insightful discussions throughout the course of this research. We also thank the editor for their dedicated guidance and the anonymous reviewers for their constructive feedback, which greatly enhanced the quality of this manuscript. The figures in this study were generated using the Generic Mapping Tools (GMT) software [28]. We express our sincere gratitude to the Geospatial Information Agency of Indonesia (BIG) and Susilo et al. [18] for providing the continuous GNSS velocity data.

References:

[1] H. Z. Abidin, H. Andreas, I. Gumilar, T. P. Sidiq, and Y. Fukuda, "Land subsidence in coastal city of Semarang (Indonesia): characteristics, impacts and causes," *Geomatics, Natural Hazards and Risk*, vol. 4, no. 3, pp. 226–240, 2013.

[2] R. Siriwardane-de Zoysa *et al.*, "The 'wickedness' of governing land subsidence: Policy perspectives from urban Southeast Asia," *PLoS One*, vol. 16, no. 6, p. e0250208, 2021.

[3] L. Pedretti, A. Giarola, M. Korff, J. Lambert, and C. Meisina, "Comprehensive database of land subsidence in 143 major coastal cities around the world: overview of issues, causes, and future challenges," *Front Earth Sci (Lausanne)*, vol. 12, p. 1351581, 2024.

[4] H. Andreas, H. Z. Abidin, D. A. Sarsito, and I. Meilano, "Investigating the tectonic influence to the anthropogenic subsidence along northern coast of Java Island Indonesia using GNSS data sets," in *E3S Web of Conferences*, 2019, p. 4005.

[5] D. Sarah, L. M. Hutasoit, R. M. Delinom, and I. A. Sadisun, "Natural compaction of Semarang-Demak Alluvial Plain and its relationship to the present land subsidence," *Indonesian Journal on Geoscience*, vol. 7, no. 3, pp. 273–289, 2020.

[6] B. D. Yuwono, H. Z. Abidin, Poerbandono, H. Andreas, A. S. P. Pratama, and F. Gradiyanto, "Mapping of flood hazard induced by land subsidence in Semarang City, Indonesia, using hydraulic and spatial models," *Natural Hazards*, vol. 120, no. 6, pp. 5333–5368, 2024.

[7] F. Kuehn *et al.*, "Detection of land subsidence in Semarang, Indonesia using persistent scatterer interferometry," in *Proceedings of Asian Association on Remote Sensing*, 2009.

[8] A. Aditiya and T. Ito, "Present-day land subsidence over Semarang revealed by time series InSAR new small baseline subset technique," *International Journal of Applied Earth Observation and Geoinformation*, vol. 125, p. 103579, 2023.

[9] S. Samieie-Esfahany, R. F. Hanssen, K. van Thienen-Visser, and A. Muntendam-Bos, "On the effect of horizontal deformation on InSAR subsidence estimates," in *Fringe 2009, Proceedings of the workshop*, 2010.

[10] F. Qu *et al.*, "Mapping ground deformation over Houston–Galveston, Texas using multi-temporal InSAR," *Remote Sens Environ*, vol. 169, pp. 290–306, 2015.

[11] P. C. Wu, M. Wei, and S. D'Hondt, "Subsidence in coastal cities throughout the world observed by InSAR," *Geophys Res Lett*, vol. 49, no. 7, p. e2022GL098477, 2022.
[12] S. Li, W. Xu, and Z. Li, "Review of the SBAS InSAR Time-series algorithms, applications, and challenges," *Geod Geodyn*, vol. 13, no. 2, pp. 114–126, 2022.
[13] K. Mogi, "Relations between the eruptions of various volcanoes and the deformations of the ground surfaces around them," *Earthquake Research Institute*, vol. 36, pp. 99–134, 1958.
[14] S. Guan, C. Wang, H. Zhang, Y. Tang, F. Wu, and L. Zou, "Inferring Subsurface Compaction from InSAR Land Subsidence Measurements Using The Mogi's Model," in *2023 SAR in Big Data Era (BIGSARDATA)*, 2023, pp. 1–4.
[15] Y. Morishita, M. Lazecky, T. J. Wright, J. R. Weiss, J. R. Elliott, and A. Hooper, "LiCSBAS: An open-source InSAR time series analysis package integrated with the LiCSAR automated Sentinel-1 InSAR processor," *Remote Sens (Basel)*, vol. 12, no. 3, p. 424, 2020.
[16] C. Yu, Z. Li, N. T. Penna, and P. Crippa, "Generic Atmospheric Correction Model for Interferometric Synthetic Aperture Radar Observations," *J Geophys Res Solid Earth*, vol. 123, pp. 9202–9222, 2018.
[17] Q. Wang, W. Yu, B. Xu, and G. Wei, "Assessing the Use of GACOS Products for SBAS-InSAR Deformation Monitoring: A Case in Southern California," *Sensors*, vol. 19, p. 3894, 2019.
[18] S. Susilo *et al.*, "GNSS land subsidence observations along the northern coastline of Java, Indonesia," *Sci Data*, vol. 10, no. 1, p. 421, 2023.
[19] M. M. Miller and M. Shirzaei, "Spatiotemporal characterization of land subsidence and uplift in Phoenix using InSAR time series and wavelet transforms," *J Geophys Res Solid Earth*, vol. 120, no. 8, pp. 5822–5842, 2015.
[20] T. Fuhrmann and M. C. Garthwaite, "Resolving three-dimensional surface motion with InSAR: Constraints from multi-geometry data fusion," *Remote Sens (Basel)*, vol. 11, no. 3, p. 241, 2019.
[21] C. Carnec and H. Fabriol, "Monitoring and modeling land subsidence at the Cerro Prieto geothermal field, Baja California, Mexico, using SAR interferometry," *Geophys Res Lett*, vol. 26, no. 9, pp. 1211–1214, 1999.
[22] T. Masterlark, "Magma intrusion and deformation predictions: Sensitivities to the Mogi assumptions," *J Geophys Res Solid Earth*, vol. 112, no. B6, 2007.
[23] W. Lo, S. N. Purnomo, D. Sarah, S. Aghnia, and P. Hardini, "Groundwater modeling in urban development to achieve sustainability of groundwater resources: A case study of Semarang City, Indonesia," *Water (Basel)*, vol. 13, no. 10, p. 1395, 2021.
[24] M. Desbrun, M. Meyer, P. Schröder, and A. H. Barr, "Implicit fairing of irregular meshes using diffusion and curvature flow," in *Proceedings of the 26th annual conference on Computer graphics and interactive techniques*, 1999, pp. 317–324.
[25] C. J. Van Der Veen and I. M. Whillans, "Flow laws for glacier ice: comparison of numerical predictions and field measurements," *Journal of Glaciology*, vol. 36, no. 124, pp. 324–339, 1990.
[26] R. Newman and N. White, "The dynamics of extensional sedimentary basins: constraints from subsidence inversion," *Philosophical Transactions of the Royal Society of London. Series A: Mathematical, Physical and Engineering Sciences*, vol. 357, no. 1753, pp. 805–834, 1999.
[27] C. Tape, P. Musé, M. Simons, D. Dong, and F. Webb, "Multiscale estimation of GPS velocity fields," *Geophys J Int*, vol. 179, no. 2, pp. 945–971, 2009.
[28] P. Wessel, W. H. F. Smith, R. Scharroo, J. Luis, and F. Wobbe, "Generic Mapping Tools: Improved Version Released," *Eos, Transactions American Geophysical Union*, vol. 94, no. 45, pp. 409–410, Nov. 2013, doi: 10.1002/2013EO450001.